EUKARYOTIC CELL, Aug. 2008, p. 1278–1288 Vol. 7, No. 8
1535-9778/08/$08.00+0 doi:10.1128/EC.00039-08

Aspergillus nidulans ArfB Plays a Role in Endocytosis and Polarized Growth▽†

Soo Chan Lee,[1]‡ Sabrina N. Schmidtke,[2] Lawrence J. Dangott,[2] and Brian D. Shaw[1]*

Program for the Biology of Filamentous Fungi, Department of Plant Pathology and Microbiology, Texas A&M University, 2132 TAMU, College Station, Texas 77843,[1] and Department of Biochemistry and Biophysics, Texas A&M University, 2128 TAMU, College Station, Texas 77843[2]

Received 1 February 2008/Accepted 29 May 2008

Filamentous fungi undergo polarized growth throughout most of their life cycles. The Spitzenkörper is an apical organelle composed primarily of vesicles that is unique to filamentous fungi and is likely to act as a vesicle supply center for tip growth. Vesicle assembly and trafficking are therefore important for hyphal growth. ADP ribosylation factors (Arfs), a group of small GTPase proteins, play an important role in nucleating vesicle assembly. Little is known about the role of Arfs in filamentous hyphal growth. We found that *Aspergillus nidulans* is predicted to encode six Arf family proteins. Analysis of protein sequence alignments suggests that *A. nidulans* ArfB shares similarity with ARF6 of *Homo sapiens* and Arf3p of *Saccharomyces cerevisiae*. An *arfB* null allele (*arfB* disrupted by a transposon [*arfB*::Tn]) was characterized by extended isotropic growth of germinating conidia followed by cell lysis or multiple, random germ tube emergence, consistent with a failure to establish polarity. The mutant germ tubes and hyphae that do form initially meander abnormally off of the axis of polarity and frequently exhibit dichotomous branching at cell apices, consistent with a defect in polarity maintenance. FM4-64 staining of the *arfB*::Tn strain revealed that another phenotypic characteristic seen for *arfB*::Tn is a reduction and delay in endocytosis. ArfB is myristoylated at its N terminus. Green fluorescent protein-tagged ArfB (ArfB::GFP) localizes to the plasma membrane and endomembranes and mutation (ArfB^{G2A}::GFP) of the N-terminal myristoylation motif disperses the protein to the cytoplasm rather than to the membranes. These results demonstrate that ArfB functions in endocytosis to play important roles in polarity establishment during isotropic growth and polarity maintenance during hyphal extension.

Polarized growth is a biological process observed for many different eukaryotic cell systems, including pollen tube formation (50), neuronal cell development (7), and fungal hyphal growth (5). Filamentous fungi are characterized by extensive polarized growth throughout most of their life cycles. This unique reliance on hyphal morphogenesis makes filamentous fungi an attractive system to study polarized growth. Invasive hyphal growth is an important strategy for animal and plant pathogenic fungi to infect and penetrate their hosts. Therefore, understanding hyphal growth will be critical to the development of therapeutic or antifungal agents.

Girbardt reported the existence of the Spitzenkörper (apical body) at growing hyphae and proposed that the Spitzenkörper coincided with the polarized growth site (18). The Spitzenkörper consists of two populations of vesicles, apical vesicles (79 to 90 nm in diameter) and microvesicles (30 to 40 nm in diameter). Microvesicles possess chitin synthesis activity and have been called "chitosomes" (4, 6). The postulated vesicle supply center thought to be necessary to explain hyphal tip growth (19, 20) may correspond with the Spitzenkörper. This has driven the hypothesis that vesicle assembly and trafficking play key roles in polarized growth in filamentous growth.

ADP ribosylation factors (Arfs) are small GTPase proteins that function in vesicle assembly and trafficking (34, 36). In *Saccharomyces cerevisiae*, Arf3 is involved in polarity establishment during budding and an *arf3* mutant shows a random budding phenotype (16, 22). The Arf3 protein localizes to cell membranes and predominantly to sites of polarized growth (22). Arf3 also genetically interacts with actin cable and actin patch components, including profilin (Pfy1), Arp2/3 complex protein (Las17p and Vrp1), formins (Bni1 and Bnr1), Arf-GTP exchange factor (Gea1), and actin-organizing proteins (Syp1 and Bud6) (30). Another function of Arf3p in yeast is in membrane trafficking during endocytosis (9, 10). ARF6, the human homolog of *S. cerevisiae* Arf3p (ScArf3p), is also involved in endocytosis, cytokinesis, and actin cytoskeleton organization (reviewed in reference 17).

Shaw et al. reported that a temperature-sensitive *N*-myristoyl transferase (NMT) mutant displayed a polarity maintenance defect in *Aspergillus nidulans* (43). Myristate from myristoyl-coenzyme A (CoA) is covalently attached to the secondary glycine of target proteins by NMT increasing in hydrophobicity (24). Myristoylated protein more readily associates with membranes or takes part in hydrophobic protein-protein interactions (24, 41). Many Arfs, including ScArf3p, are N myristoylated (2, 35). We hypothesized that Arf proteins may be the direct connection between N myristoylation and polarized cell morphogenesis in filamentous fungi. Indeed, in *S. cerevisiae*, N-myristoylated Arfs, including Arf1p, Arf2p,

* Corresponding author. Mailing address: Program for the Biology of Filamentous Fungi, Department of Plant Pathology and Microbiology, Texas A&M University, 2132 TAMU, College Station, TX 77843. Phone: (979) 862-7518. Fax: (979) 845-6483. E-mail: bdshaw@tamu.edu.

† Supplemental material for this article may be found at http://ec.asm.org/.

‡ Present address: Department of Molecular Genetics and Microbiology, Duke University Medical Center, 320 Carl Building, Box 3546, Durham, NC 27710.

▽ Published ahead of print on 6 June 2008.

TABLE 1. Strains used in this study

Strain name	Description	Source or reference
A773	*pyrG89 wA3 pyroA4 veA1*	FGSC
A4	Wild type	FGSC
TN02A7	*pyrG89 pyroA4 riboB2 nkuA*::*argB*	37
BTN1	*pyrG89 pyroA4 riboB2 nkuA*::*argB arfB*::Tn::*pyr-4*	This study
WB17	*pyrG89 wA3 pyroA4 arfB*::*sGFP*::*pyr-4 veA1*	This study
MB13	*pyrG89 wA3 pyroA4 arfB^{G2A}*::*sGFP*::*pyr-4 veA1*	This study
ASUAGA4	*pyrG89 argB1 pyroA4 riboB2 actA*::*GFP*::*argB*	53
BAC1	*arfB*::Tn::*pyr-4 actA*::*GFP*::*argB*	This study

TABLE 2. Plasmids used in this study

Plasmid name	Description	Source or reference
pGEM-T Easy vector	TA cloning vector for PCR product cloning	Promega
pGEM-arfB	*arfB* in pGEM-T Easy vector	This study
pENTR	Entry vector for gateway cloning	Invitrogen
pArfB-entry	*arfB* in pENTR	This study
pArfB^{G2A}-entry	*arfB^{G2A}* in pENTR	This study
pGEM-pyr4	*pyr-4* in pGEM-T Easy vector	This study
pMT-sGFP	Gateway destination vector with *argB* gene	51
pSL-sGFP	Gateway destination vector with *pyr-4* gene	This study
pArfB::GFP-pyr4	pSL-sGFP with *arfB*::*sGFP* replacing the *ccdB* box	This study
pArfB^{G2A}::GFP-pyr4	pSL-sGFP with *arfB^{G2A}*::*sGFP* replacing the *ccdB* box	This study

Arf3p, and Arl1p, have been shown to be associated with polarized budding, in which Arf1p, Arf2p, and Arl1p are involved in a secretion pathway through the Golgi network (40, 46). These secretory vesicles may be destined for the Spitzenkörper in filamentous fungi.

In this study we found six Arf family proteins in *A. nidulans*. Three, namely, AN1126.3, AN5020.3, and AN5912.3 (ArfA, ArfB, and ArlA, respectively), are predicted to be myristoylated (31). Overexpression of ArfA has been shown to suppress the *swoF* myristoylation mutant (32). Here ArfB is investigated further, since it is the putative ortholog of Arf3p in *S. cerevisiae* associated with polarized bud site selection (22) and actin organization (11, 30). We show that ArfB is important for the establishment and maintenance of hyphal polarity, possibly by directing endocytosis in *A. nidulans*, and that this role requires N myristoylation of the protein.

MATERIALS AND METHODS

Strains, growth condition, plasmids, media, and reagents. *A. nidulans* strains and plasmids used in this study are listed in Tables 1 and 2, respectively. The plasmids were maintained in *Escherichia coli* XL1-Blue (Stratagene, La Jolla, CA) and manipulated as previously described (42). *E. coli* DB3.1 was used for the propagation of plasmids containing the *ccdB* box. *E. coli* CC118 was used for the propagation of the transposon donor plasmid containing the R6K replication origin. Complete and minimal media for *A. nidulans* were prepared as described previously (27). All chemicals for media, buffer, and supplements were purchased from Sigma (St. Louis, MO) unless otherwise indicated.

Disruption of *arfB* by a transposon. The *arfB* gene was PCR amplified from 500 bp upstream of the start codon and 451 bp downstream of the stop codon by use of the following primers: 5020F (5′-GGGGTACCCCGGCTCGTGGGCG CGCTGAGT-3′) and AN5020TNR (5′-ACGGCATAACATGACGGAAT-3′). The amplicon was cloned into the pGEM-T Easy vector (Promega, Madison, WI) to produce pGEM-*arfB*. A transposon insertional mutagenesis strategy (37) was used to disrupt the *arfB* gene. This transposon contains the *Neurospora crassa pyr-4* gene as a selectable marker. In-frame insertion of the transposon was verified by PCR. The exact insertion site was determined by sequencing with primers N and S from the GPS-1 kit (New England Biolabs Inc., Ipswich, MA). pArfBTn2, carrying the transposon in the first predicted intron of the *arfB* (after 139 bp from the start of the gene) in the vector pGEM-*arfB*, was linearized with SphI (New England Biolabs Inc., Ipswich, MA), which cuts the plasmid outside of the *arfB* gene. The linearized plasmid was transformed using previously described methods (43) into *A. nidulans* strain TN02A7 (Table 1). This strain is disrupted at *nkuA* to enhance homologous recombination (37). We named the disrupted strain BTN1 (Table 1).

Green fluorescent protein (GFP) tagging of ArfB and ArfB^{G2A}. The intact *arfB* gene was amplified from wild-type strain A4 genomic DNA with the following primers: GarfBF (5′-CACCATGGGCGGCTCAGTGTCGAA-3′; underlining indicates the secondary glycine) and GarfBR (5′-TTTTTGGGGTTGTTGGAC CT-3′). To generate nonmyristoylated ArfB, a site-directed mutation was introduced by using primer mGarfBF (5′-CACCATGGCCGGCTCAGTGTCGAAG AT-3′) instead of GarfBF, which changed the secondary glycine into alanine (G2A; the site of this change is underlined). The secondary glycine is critical for myristoylation (33). The *arfB* and *arfB^{G2A}* amplicons were cloned into the gateway entry vector pENTR (Invitrogen, Carlsbad, CA) to produce pArfB-entry and pArfB^{G2A}-entry, respectively.

To construct a GFP expression vector with the *pyr-4* marker gene, pMT-sGFP (51) was partially digested with NotI (New England Biolabs Inc., Ipswich, MA) and the vector fragment without the 1.8-kb fragment containing the *argB* gene was ligated with a 1.6-kb fragment containing the *pyr-4* gene from pGEM-pyr4 to produce pSL-sGFP (Table 2).

The *ccdB* box in pSL-sGFP was exchanged with *arfB* or *arfB^{G2A}* in the entry vectors mentioned above through the use of a LR Clonase reaction following the manufacturer's instructions (Invitrogen, Carlsbad, CA) to generate pArfB::sGFP-pyr4 or pArfB^{G2A}::sGFP-pyr4, respectively. Each vector was transformed into A773 (Table 1) or TN02A7. pArfB::sGFP-pyr4 was also transformed into AXL18, an NMT mutant (43), to observe the localization pattern of ArfB::GFP in the absence of N myristoylation.

Southern, Northern, and Western blotting. The intact *arfB* gene amplified with primers GarfBF and GarfBR was used as the probe for Southern and Northern blotting. The probe was labeled by using Prime-It II, a random-primer labeling kit (Stratagene, La Jolla, CA), by using [γ-^{32}P]CTP. For Southern blotting, the wild-type strain (TN02A7) and BTN1 (Table 1) genomic DNAs were digested with SphI and separated on a 1% agarose gel. For Northern blotting, total RNA from the wild-type strain and BTN1 was extracted after 24 h of incubation in liquid culture by using Trizol reagent (Invitrogen, Carlsbad, CA) as indicated by the instruction of the manufacturers. The RNA was separated on a 1% agarose gel containing 2.2 M of formaldehyde. Standard procedures for Southern and Northern blotting were followed (42).

Monoclonal anti-GFP antibody (Santa Cruz Biotechnology, Inc., Santa Cruz, CA) was used for Western blotting for GFP-tagged proteins. Total proteins were extracted from WB17 and MB13 (*arfB*::GFP and *arfB^{G2A}*::GFP, respectively; Table 1) and separated on a precast 12% sodium dodecyl sulfate-polyacrylamide gel electrophoresis gel (Bio-Rad, Hercules, CA). Protein extraction and Western blotting were performed as previously described (31).

MALDI-TOF MS. Proteins for matrix-assisted laser desorption ionization–time of flight mass spectrometry (MALDI-TOF MS) analysis were prepared by immunoprecipitation. From a total protein preparation prepared as previously described (31), ArfB::GFP proteins were selectively bound to the monoclonal anti-GFP antibody (see above) and the antibody-protein complexes were precipitated with protein A in the ImmunoPure immobilized protein A system (Pierce Biotechnology, Inc., Rockford, IL) following the company's instructions. Sodium dodecyl sulfate gel electrophoresis (29) of the precipitated proteins was performed and the gels were stained with Bio-Safe Coomassie blue (Bio-Rad, Hercules, CA). A band corresponding to the ArfB::GFP protein was excised from the gel and subjected to reduction, alkylation with iodoacetamide, trypsin digestion (Promega, Madison, WI), and extraction according to established methods (45). The extracted peptides were purified using C_{18} ZipTip (Millipore) and eluted directly onto the sample plate by use of 2 μl of α-cyanohydroxy-

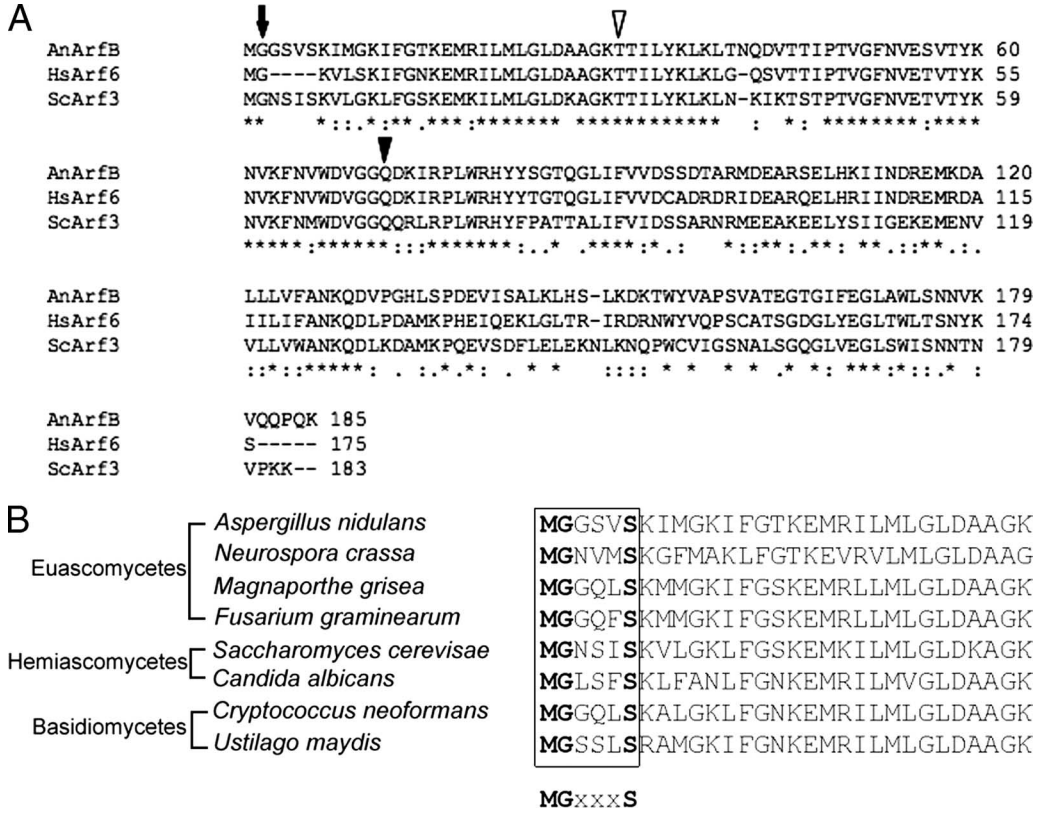

FIG. 1. Similarity in amino acid sequences of ArfB (*A. nidulans*), Arf3p (*S. cerevisiae*), and ARF6 (*Homo sapiens*) and the N termini of ARF6 family proteins from representative fungi. (A) Alignment of protein sequences of AnArfB, ScArf3p, and HsARF6. Arrow, N-myristoylation motif; empty arrowhead, GTP binding site; black arrowhead, GTP hydrolysis site. (B) N-terminal 30-amino-acid sequences of ARF6 family proteins of *A. nidulans* (AN5020.3), *N. crassa* (NCU07173.1), *M. grisea* (MGG10676), *F. graminearum* (FG04483.1), *S. cerevisiae* (Arf3p), *C. albicans* (CaO19.5964), *C. neoformans* (CNL06630), and *U. maydis* (UM05580.1). All fungal ARF6 orthologs examined contain the consensus N-myristoylation motif (M-G-x-x-x-S-).

cinammic acid solution (6 mg/ml in 50% [vol/vol] acetonitrile containing 0.1% trifluoroacetic acid). Mass spectra were collected in reflectron positive-ion mode on an Axima CFR MALDI-TOF MS (Shimadzu/Kratos, Manchester, United Kingdom). The peptide masses were calibrated internally with trypsin fragments. Average mass differences between predicted and measured masses were between 20 and 300 ppm.

Microscopy. GFP protein and FM4-64-stained live cells were visualized in germlings grown in custom-made aluminum chambers designed for live-cell imaging of fungal cells (28). For time-lapse imaging, an Olympus BX51 microscope (Olympus America Inc., Melville, NY) was outfitted with a Prior shutter to limit phototoxicity to the cells. Simple PCI software (version 5.3.1.081004; Compix Inc., Imaging Systems, Cranberry Township, PA) was used to acquire images of growth at 30-second intervals. To observe the endocytosis process in cells, wild-type and BTN1 cells were grown on a coverslip submerged in liquid complete medium. After 24 h of incubation, fresh medium containing 12.5 μM of FM4-64 was replaced with the growing medium lacking the dye. The coverslip with cells was overlaid on the aluminum chamber. A narrow-band G-excitation filter with 530 to 550 nm of excitation and 590 nm of emission (Olympus America Inc., Melville, NY) was used to obtain FM4-64 fluorescent images. Microscopic observation for GFP and all image processing were conducted as previously described (44, 52).

RESULTS

ArfB is an ARF6 family protein in *A. nidulans*. *A. nidulans* and *S. cerevisiae* encode six Arf family proteins (ArfA [AN1126.3], ArfB [AN5020.3], ArlA [AN5912.3], AN3934.3, AN0411.3, and AN0634.3 for *A. nidulans*) and Arf1p, Arf2p, Arf3p, Arl1p, Sar1p, and Arl3p for *S. cerevisiae* (see Fig. S1 in the supplemental material). We found that ArfB (AN5020.3) is a putative ortholog of ScArf3p, which was previously shown to be involved in the selection of bud sites (22) through interactions with proteins involved in actin assembly (30). *A. nidulans* ArfB (AnArfB) and ScArf3p are further grouped into the ARF6 family of proteins (or class III Arfs), named after human ARF6 (17). The AnArfB, ScArf3p, and *Homo sapiens* ARF6 (HsARF6) protein sequences were aligned (Fig. 1A). AnArfB shares 59% amino acid sequence identity with ScArf3p and 72% identity with HsARF6. ScArf3p shares 59% similarity with HsARF6. The AnArfB, ScArf3p, and HsARF6 proteins have a conserved N-terminal myristoylation site and a conserved GTP binding and hydrolysis site for their GTPase activity (Fig. 1A). The *arfB* gene is located on chromosome III from bp 507,503 to bp 508,272 on contig 84 (of release 3 of the *A. nidulans* genome database [http://www.broad.mit.edu/annotation/genome/aspergillus_group/MultiHome.html]). The *arfB* gene is 770 bp in length and is predicted to contain four introns at the following positions: 94 to 153 bp, 312 to 363 bp, 511 to 561 bp, and 674 to 725 bp. ARF6 family proteins were retrieved from filamentous fungal genome databases including protein data for *A. nidulans*, *N. crassa*, *Magnaporthe grisea*, *Fusarium graminearum*, *Candida albicans*, *Cryptococcus neoformans*, and *Ustilago maydis* in addition to *S. cerevisiae*. All of these proteins contain the consensus Met-Gly-x-x-x-Ser/Thr motif

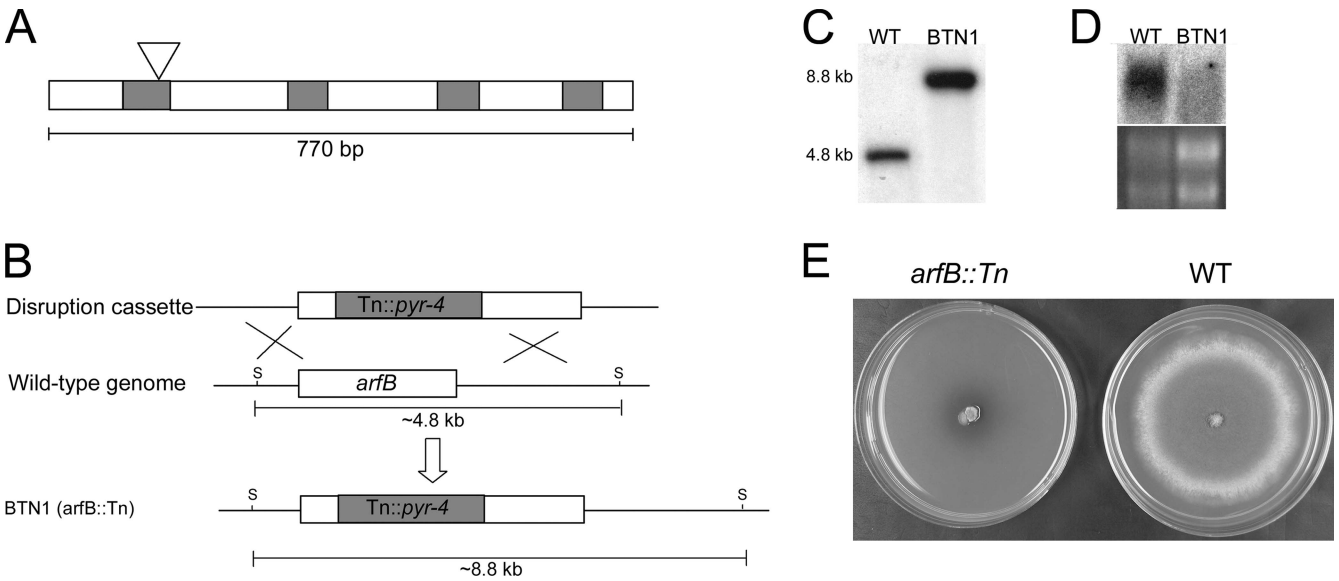

FIG. 2. Disruption of *arfB* gene and colony phenotype. (A) Position of the transposon insertion site in the *arfB* disruption construct. Gray boxes are predicted introns. The triangle indicates the transposon insertion site. (B) The disruption construct homologously replaced the native *arfB* locus to create the BTN1 (*arfB*::Tn) strain. S, SphI recognition site. (C) Southern blot analysis of the wild type (WT) and of BTN1 indicates that a single copy of the *arfB*::Tn cassette replaced the native *arfB* locus in the BTN1 strain. (D) Northern blot analysis shows that the transposon insertion in the predicted first intron disrupted the expression of the *arfB* gene. (E) BTN1 colonies develop markedly slower than do those of the wild type.

(established in reference 24) at their N termini (Fig. 1B), suggesting that N myristoylation of ARF6 family proteins is important for their function.

Disruption of *arfB* by a transposon insertion. To investigate the role of *arfB* in *A. nidulans*, we disrupted the gene. The *arfB* disruption cassette was constructed in the pGEM-T Easy vector (see Materials and Methods). The transposon contains the *N. crassa pyr-4* gene as a nutritional selection marker. Sequencing verified the transposon insertion site in the predicted first intron of the *arfB* gene (after 139 bp from the start of the gene) (Fig. 2A), resulting in a truncation upstream of the GTP binding and hydrolysis sites. The intact *arfB* gene was replaced by transformation in the *nkuA* deletion strain (TN02A7) (Fig. 2B). A single insertion was verified by PCR (data not shown). Southern blot analysis showed that the *arfB* disruptant (BTN1) has an 8.8-kb band that is upshifted relative to the approximately 4.8 kb of the control strain. This indicates that the BTN1 strain contains a single copy of the *arfB*::Tn cassette (Fig. 2C) within the *arfB* gene. We were unable to generate protoplasts from the disruption strain to complement it by transformation with the intact *arfB* gene. This is due both to its impaired growth and to its thickened cell walls (see below). Therefore, we confirmed that observed phenotypes were due to the disruption of the *arfB* locus and not due to a second site mutation introduced by transformation by backcrossing BTN1 to the wild-type strain. In this backcross, we obtained progeny with a segregation ratio of 1:1 ($n = 153$; 74:79, mutant phenotype:wild-type phenotype). We confirmed that four independent progeny displayed a phenotype identical to that of BTN1 and contained the *arfB*::Tn cassette at the *arfB* locus (data not shown). Therefore, strain BTN1 and its progeny contain one homologous insertion of *arfB*::Tn, and the disruption of the *arfB* gene resulted in the abnormal phenotype.

Since the transposon is in a predicted intron, we examined the expression of the *arfB* gene in the control strain and the *arfB*::Tn strain. A Northern blot (Fig. 2D) shows that the control strain expressed intact mRNA of *arfB*; from *arfB*::Tn, however, the *arfB* mRNAs were below the detection limit (Fig. 2D), indicating that the transposon insertion disrupts the expression of the *arfB*. We therefore conclude that *arfB*::Tn is a null allele.

Compared to the control strain, the *arfB*::Tn strain produced slow-growing colonies that are aconidial (Fig. 2E). The lack of conidiation was partially suppressed in the presence of an osmotic stabilizer (1.2 M sorbitol), though colonial growth remained limited (data not shown). This characteristic allowed the propagation of the *arfB*::Tn disrupted strain by conidia.

The *arfB*::Tn strain is defective in polarity establishment during spore germination and polarity maintenance during hyphal growth. The *arfB*::Tn strain displayed extended isotropic growth, multiple germ tube emergence, and dichotomous branching at hyphal apices (Fig. 3). Under identical conditions, the wild-type strain sent a primary germ tube following isotropic growth and a secondary germ tube (Fig. 3A). Using time-lapse image acquisition, we compared the *arfB*::Tn strain to the wild-type strain during spore germination and the establishment of hyphal growth. The wild-type strain grows isotropically (Fig. 3B; also see Movie S1 in the supplemental material) and then establishes a polarization site. After primary germ tube formation, the secondary germ tube emerges approximately 180 degrees from the primary germ tube, and then the primary germ tube becomes septated (see Movie S2 in the supplemental material). However, in the *arfB*::Tn strain, extended isotropic growth gives rise to a swollen conidium of up to approximately 20 μm in diameter (Fig. 3B; also see Movie S3 in the supplemental material). After an extended isotropic growth period, the *arfB*::Tn strain displays the following three different phenotypic variations (Fig. 3B; also see Movie S4 in the sup-

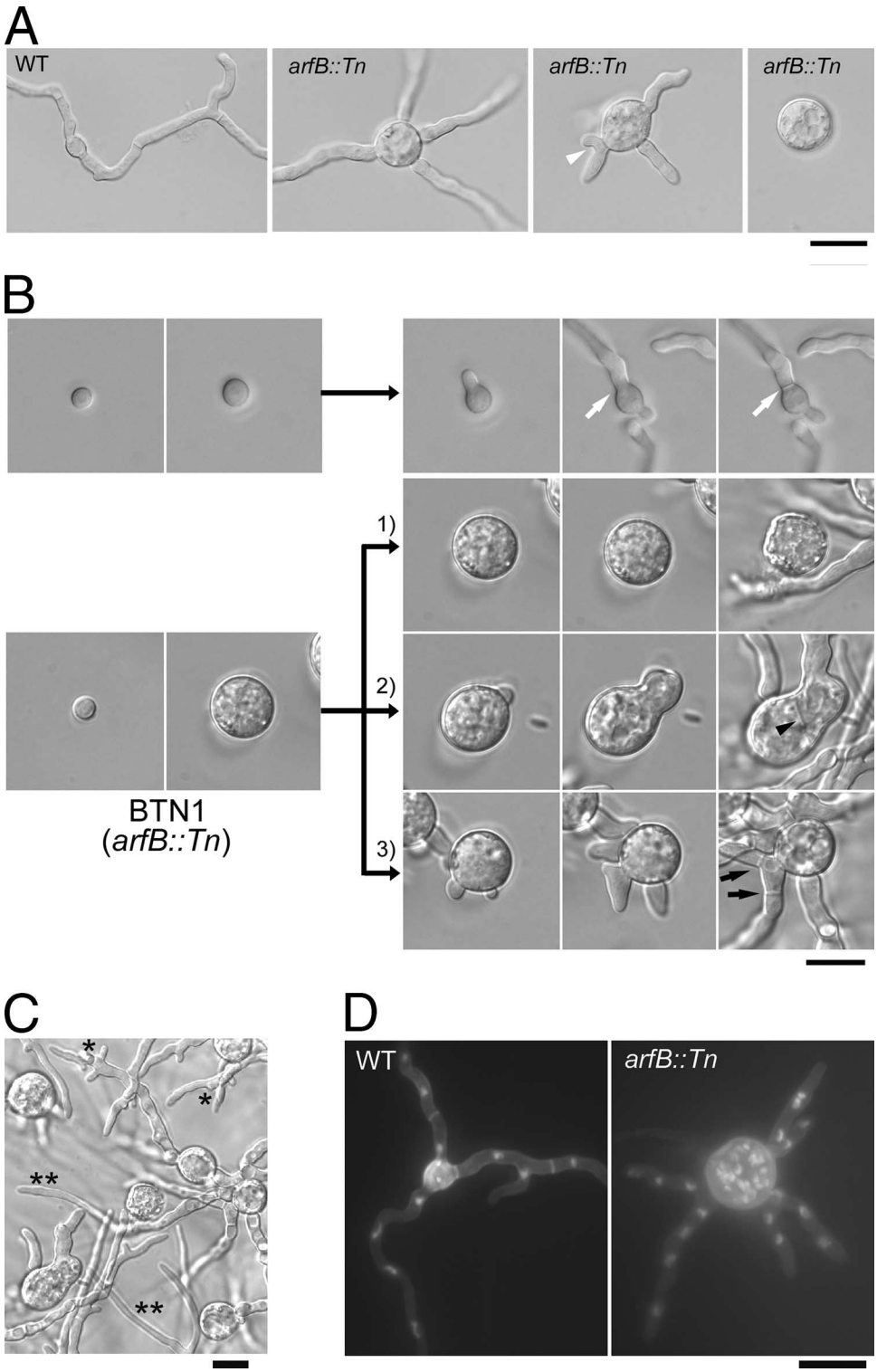

FIG. 3. Phenotype of the *arfB*::Tn strain. (A) Microscopic phenotypes of the wild-type (WT) and *arfB*::Tn strains. A site where multiple germ tubes emerge from the same conidium is indicated by a white arrowhead. (B) Time-lapse images of wild-type and BTN1 cells. The white arrows indicate septation sites, the black arrowhead indicates a septum, and the black arrows indicate simultaneous septation sites for the *arfB*::Tn strain. (C) Polarized hyphal growth of the *arfB*::Tn strain. Symbols: *, abnormal hyphal growth of the *arfB*::Tn strain; **, wild-type-like hyphal growth of the *arfB*::Tn strain. (D) Combined Z-stack images from a spinning-disc confocal microscope of the wild-type and *arfB*::Tn strains. Multiple nuclei in the isotropic, apolar conidium are observed for the *arfB*::Tn strain. Germlings of the wild-type and *arfB*::Tn strains were stained with calcofluor to visualize cell walls and with Hoechst 33258 to visualize nuclei. Numerical aperture (NA), 1.4 with oil. Bars = 20 μm.

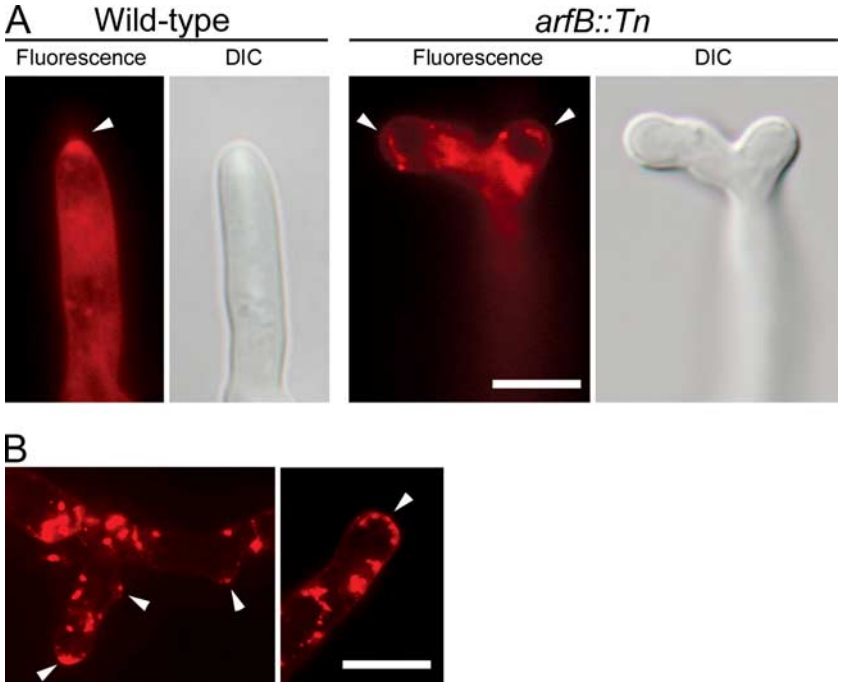

FIG. 4. Wild-type and *arfB*::Tn strains stained with FM4-64. (A) Wide-field fluorescence images of intact Spitzenkörper in wild-type strains and the lack of FM4-64-stained Spitzenkörper in apices undergoing tip splitting in the *arfB*::Tn strain. These apices often exhibited diffuse FM4-64-stained structures with multiple foci. DIC, differential interference of contrast. (B) Confocal microscopic images of hyphal apices of the *arfB*::Tn strain. FM4-64-stained structures are diffuse and/or contain multiple foci. White arrowheads indicate these apical bodies. NA, 1.4 with oil. Bars = 5 μm.

plemental material). (i) Large isotropically swollen conidia lyse (35.3% ± 3.7%; n = 607.). (ii) Large isotropically swollen conidia send a germ tube, followed by the loss of polarity of the germ tube (17.2% ± 4.4%). These apolar germ tubes can later recover polarity to produce additional germ tubes. (iii) Multiple germ tubes emerge simultaneously from the swollen conidium (47.5% ± 3.7%). Hyphae often dichotomously split at their apices. Multiple simultaneous septation events were observed in dichotomously branching hyphae (Fig. 3B). Initial hyphal growth is consistently irregular. Hyphae meandered and produce irregularly lobed cells (Fig. 3C). Interestingly, hyphae later (after 60 to 80 μm of initial hyphal growth) appear almost like wild-type hyphae, suggesting that another gene may function to compensate for the absence of *arfB* or that the gene functions primarily during the initial stages of hyphal growth. Germlings of the wild-type and *arfB*::Tn strains were stained with calcofluor to visualize cell walls and with Hoechst 33258 to visualize nuclei (Fig. 3D). Multiple nuclei in cell compartments of the *arfB*::Tn strain indicated no cell cycle-associated phenotypes.

The Spitzenkörper of the wild-type strain (A4) and that of the *arfB*::Tn strain were examined. The Spitzenkörper is a filamentous fungus-specific "organelle" composed of a cloud of secretory vesicles and involved in hyphal growth (20). We visualized the Spitzenkörper by staining with FM4-64 (13). The wild-type strain has an intact Spitzenkörper at the hyphal apex (Fig. 4A); however, the *arfB*::Tn strain lacks an intact FM4-64-stained Spitzenkörper. These strains sometimes exhibited multiple FM4-64-stained diffuse apical bodies at the dichotomously splitting tip (Fig. 4B). Hyphae with irregular branches and irregular hyphal apices also lacked an intact FM4-64-stained Spitzenkörper (Fig. 4B). It is possible that trafficking of the dye in the *arfB* mutant caused insufficient staining of the Spitzenkörper or that intact ArfB is required to assemble a wild-type Spitzenkörper.

ArfB is involved in endocytosis. To verify the function of ArfB in endocytosis in *A. nidulans*, we stained live cells of the wild-type and *arfB*::Tn strains with FM4-64 and tracked the uptake of the dye over time. In the wild-type strain, similar to previous observations (38), the dye appeared on the plasma membrane within 10 min after treatment. After 45 min, the dye was taken up by cells and localized to endomembranes, which may be mature endosomes or vacuoles (Fig. 5A and B). In the *arfB*::Tn strain, dye uptake was delayed. After 30 min of treatment, the dye remained on the plasma membrane. Even after 60 min or more of treatment, the labeling of endomembrane was diffuse in the *arfB*::Tn strain in comparison with what was seen for the wild type (Fig. 5B).

Actin patches are thought to be sites of endocytosis (26). Therefore, we also observed actin patches in the wild-type and *arfB*::Tn strains. Our lab has previously constructed ActA::GFP (actin) (53) in which actin localized to cortical patches. To obtain an *arfB*::Tn strain expressing ActA::GFP, we crossed ASUAGA4 (*actA*::*GFP*) to BTN1 (*arfB*::Tn). Progeny displaying the *arfB*::Tn phenotype were examined for the expression of ActA::GFP. In wild-type cells, actin patches were concentrated at growing hyphal apices (Fig. 6A). In the *arfB*::Tn cells, however, the actin patches were dispersed randomly throughout apolar cells, while in polarized cells the actin patches were enriched at hyphal apices (Fig. 6B), indicating

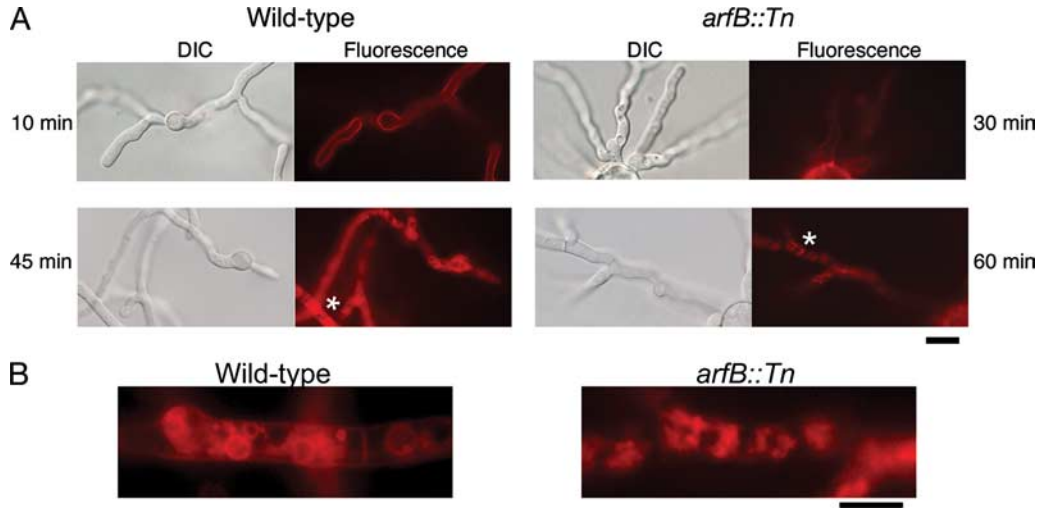

FIG. 5. Monitoring of endocytosis with FM4-64 staining in the wild-type and *arfB*::Tn strains. (A) Movement of FM4-64 into the wild-type and *arfB*::Tn cells. Uptake is delayed in *arfB*::Tn cells. NA, 1.4 with oil. Bar = 20 μm. (B) Hyphae of the wild-type and *arfB*::Tn strains in panel A (asterisk) after 45 min and 60 min, respectively, of treatment with FM4-64 were enlarged. Endomembranes appear compromised in *arfB*::Tn cells. DIC, differential interference of contrast. NA, 1.4 with oil. Bar = 5 μm.

that the localization of actin patches at the hyphal apex was delayed in the mutant.

ArfB::GFP localization. To observe the localization of ArfB, expression constructs driven by the alcohol-inducible *alcA* promoter (14) were assembled for ArfB::GFP and ArfB^{G2A}::GFP. These constructs were ectopically inserted in the wild-type A773 strain. Western blotting with monoclonal anti-GFP antibody showed a single band from total proteins of WB17 and MB13 that were expressed at comparable levels (*arfB*::*sGFP* and *arfB*^{G2A}::*sGFP*, respectively) (see Fig. S2 in the supplemental material), indicating that the GFP localization reported below was not caused by free GFP. ArfB::GFP localized to the plasma membrane, to septa, and to endomembranes, which may be endoplasmic reticulum, vacuoles, or endosomes (Fig. 6C and E). ArfB::GFP could be endocytosed to internal membranes through membrane recycling. It is not surprising that membrane proteins are internalized through endocytosis (15, 21). It is also possible that the endomembrane localization could be caused by the *alcA*-driven overexpression of ArfB::GFP protein. ArfB::GFP was not enriched in the plasma membranes at the hyphal tip (Fig. 6D). Plasmolysis of labeled cells indicated that ArfB::GFP is not on the septum wall but rather on the plasma membrane at the septum (Fig. 6F). Because septa have plasma membrane on both sides of the wall, they were brighter than membrane along other regions of the hyphae. ArfB::mRFP (monomeric red fluorescent protein) showed a similar localization pattern (data not shown). Four different strains with genotypes of *alc*(*p*)::*arfB*::*GFP arfB*::Tn or *alc*(*p*)::*arfB mRFP arfB*::Tn showed wild-type hyphal growth in the presence of ArfB::GFP or ArfB::mRFP expression under *alcA*-inducing conditions, demonstrating that both ArfB::GFP and ArfB::mRFP are functional (see Fig. S3 in the supplemental material).

To elucidate the role of N myristoylation in the localization of ArfB, we constructed a nonmyristoylated form of ArfB by mutating the secondary glycine to alanine (G2A). ArfB^{G2A}::GFP localized to the cytoplasm (Fig. 6C). We also expressed ArfB::GFP in the *swoF1* NMT mutant (43), where its localization was cytoplasmic (Fig. 6C). Multiple independent transformants with the *arfB*::*sGFP* (12 transformants) and *arfB*^{G2A}::*sGFP* (5 transformants) constructs displayed the same localization pattern (data not shown). Thus, the elimination of the myristoylation motif completely disrupts the localization of ArfB. This result demonstrates that N myristoylation of ArfB is required for the proper localization of the protein.

ArfB::GFP is N myristoylated. We overexpressed ArfB::GFP from wild-type strains. After total protein extraction, the GFP-tagged protein was selectively purified by immunoprecipitation using monoclonal anti-GFP antibody (Santa Cruz Biotechnology, Inc., Santa Cruz, CA). The immunoprecipitated ArfB::GFP was approximately 47 kDa (Fig. 6A). The band was differentiated from the heavy chain (50 kDa) of the GFP antibody (data not shown). The band was excised from polyacrylamide gel; subjected to reduction, alkylation, and trypsin digestion; and analyzed by MALDI-TOF MS.

N-terminal myristoylation occurs at the secondary glycine after cleavage of the leading methionine (25). Therefore, various isoforms of ArfB::GFP could be generated. Theoretical monoisotopic masses for ArfB::GFP are summarized in Table 3. Each of the identified peaks showed the expected isotope patterns characteristic of peptides (data not shown). In the case of the wild-type ArfB::GFP, a peak was observed at the *m*/*z* value of 744.6550 (Fig. 7). This value is in good agreement with the theoretical value of the amino-terminal peptide of ArfB with the addition of myristoyl-CoA (744.6682) with the methionine absent. A leading methionine is cleaved and secondary glycine is myristoylated, as demonstrated previously (24). This result demonstrates that ArfB is myristoylated.

DISCUSSION

One of the long-term goals of our lab is to better understand how N myristoylation plays a role in polarized cell morphogenesis in *A. nidulans*. Indeed, the temperature-sensitive

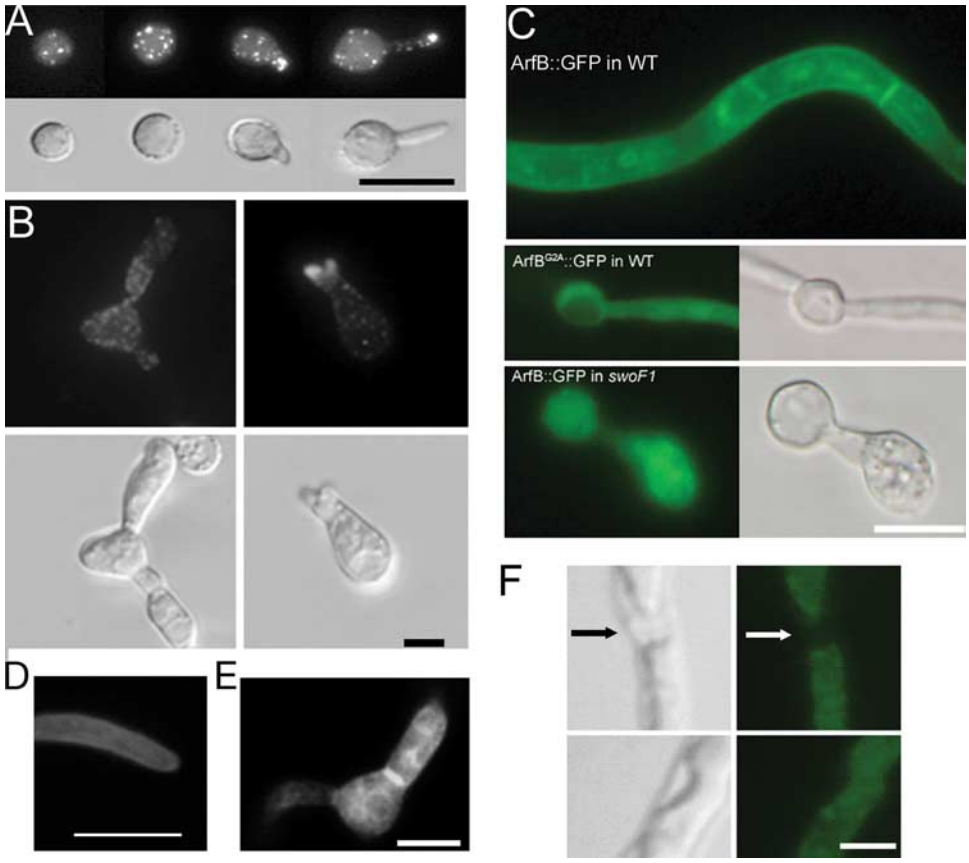

FIG. 6. Localization of actin patches in the wild-type and *arfB*::Tn strains and localization of ArfB::GFP and Arf^{G2A}::GFP. (A and B) Combined wide-field Z-stack images of actin::GFP patches in the wild-type (A) and in the *arfB*::Tn (B) strains. Cells were imaged by differential interference of contrast (DIC). Actin patches are concentrated near polarized hyphal apices in wild-type and polarized *arfB*::Tn cells but are random in apolar mutant cells. (C) Localization of ArfB::GFP and ArfB^{G2A}::GFP in wild-type (WT) cells shown by wide-field fluorescence. ArfB::GFP localizes prominently to septa and to plasma membrane. ArfB^{G2A}::GFP localization is diffused in the cytoplasm. ArfB::GFP localization in the *swoF1* strain (the NMT mutant) is cytoplasmic. (D) Confocal microscopic image of ArfB::GFP at a hyphal apex. ArfB::GFP localizes to the cell membrane. (E) Wide-field fluorescence image of ArfB::GFP on endomembranes, visualized by increasing the exposure relative to that used for panel C. (F) DIC image (left) and wide-field fluorescence image (right) of ArfB::GFP after plasmolysis. Arrows indicate a septum; ArfB::GFP does not persist on septal walls after plasmolysis. NA, 1.4 with oil. Bars = 5 μm (B and F) and 10 μm (A, C, and D).

swoF1 mutant, containing a mutation in the NMT, displayed abnormal polarized growth at the restrictive temperature (43). When grown in submerged culture at restrictive temperature, the *swoF1* mutant first grows isotropically and then sends a germ tube that is similar to the wild-type germ tube. Immediately after this germ tube emerges, hyphal growth ceases and the tip swells isotropically. Previously we found that NMT regulates 26S proteasome activity during early polarized morphogenesis and established the myristoylome of *A. nidulans* with 41 predicted myristoylated proteins (31). We have also demonstrated that overexpression of ArfA partially suppresses the polarity phenotype of the *swoF* myristoylation mutant (32). The exact role of NMT in polarized growth in systems including *S. cerevisiae*, filamentous fungi, and mammalian cells remains to be fully elucidated.

TABLE 3. Predicted mass value of N-terminal tryptically digested fragment of ArfB::GFP

Mass value	Position	Modification(s)	Modified mass value	Peptide sequence	Protein
665.33[a]	1–7	MSO[c]	681.32	MGGSVSK	ArfB
	1–7	MYR[d]	875.71		ArfB
	1–7	MSO + MYR	891.70		ArfB
534.29[b]	2–7	MYR	744.67	GGSVSK	ArfB

[a] Theoretical mass value of unmodified N-terminal fragment of ArfB::GFP.
[b] Theoretical mass value of unmodified N-terminal fragment of ArfB::GFP after cleavage of methionine.
[c] MSO, addition of methionine sulfoxide (artificial modification).
[d] MYR, N myristoylation.

In filamentous fungi, the Spitzenkörper directs hyphal polarized growth (18). The Spitzenkörper consists of a cloud of vesicles and has been considered a vesicle supply center (19, 20). Since Arfs are involved in coated vesicle formation and trafficking and many Arfs are N myristoylated (2, 34–36), they could link N myristoylation to polarized growth in the filamentous fungi.

A comparative genome analysis of *A. nidulans* and *S. cerevisiae* revealed that both organisms encode six Arf family proteins (see Fig. S1 in the supplemental material). In a previous study using yeast, Arf3p has been shown to be involved in

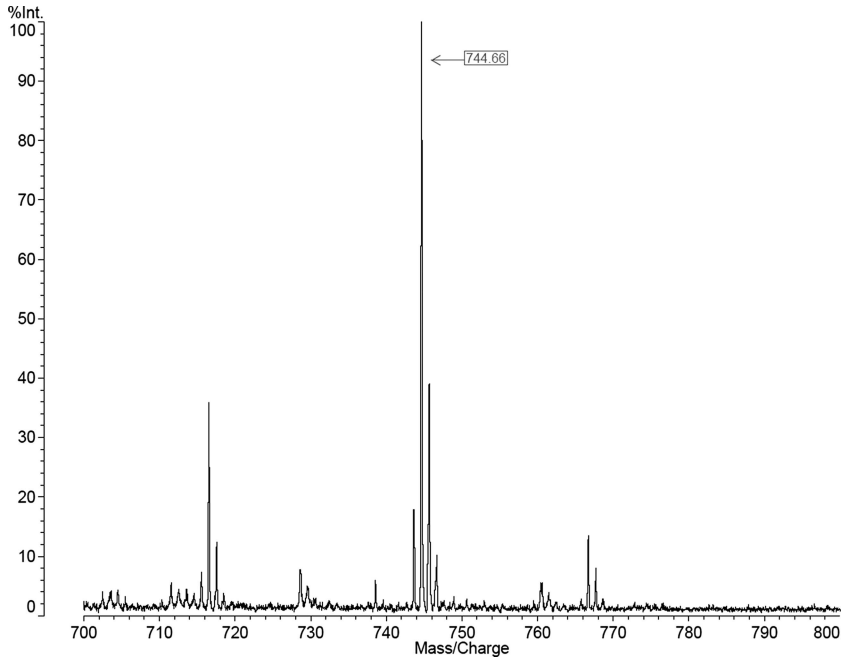

FIG. 7. MALDI-MS of ArfB after tryptic digestion. The peak at the *m*/*z* value of 744.6550 indicates that ArfB::GFP is myristoylated, as calculated (*m*/*z* = 744.6682) in Table 3. %Int, percent intensity.

developing polarity during bud formation (22) and in actin cytoskeleton organization (30). ArfB (AN5020.3) of *A. nidulans* shares close similarity with Arf3p (Fig. 1A) and both proteins have a conserved N-myristoylation motif. ArfB and Arf3p are further classified into the ARF6 protein family (named for human ARF6), and many filamentous fungal ARF6 family proteins contain a conserved consensus N-myristoylation motif (Fig. 1B). ArfB, therefore, may be one of the connections between N myristoylation and polarized cell morphogenesis.

Disruption of the *arfB* gene resulted in defects in polarized morphogenesis (Fig. 3). The ArfB disruptant displayed extended isotropic growth upon spore germination, leading to apolar cells of up to 20 μm in diameter. In contrast, wild-type conidia grow isotropically to no more than 5 μm of diameter before sending out a germ tube (Fig. 3B). The loss of polarity without cell cycle arrest (Fig. 3D) is similar to what is seen for other polarity-defective mutants examined in our lab (43, 44, 52). After the isotropic growth stage, approximately 48% of the *arfB* mutant germlings sent germ tubes (Fig. 3A and B). Previously, it was observed that delivery of active Cdc42 to an artificial polar site triggers a spontaneous polarization without polarity determinants in *S. cerevisiae* (55). Our data also show that *A. nidulans* is likely to polarize spontaneously after the abnormal swellings without the function of ArfB through an as-yet-undetermined mechanism.

Arf3 participates in actin organization in *S. cerevisiae* (30). We have shown that in the *arfB* mutant, the actin cytoskeleton is not organized properly in apolar cells but that the apical concentration of actin patches is restored in polarized cells. Therefore, random actin distribution at the initial stage of polarity establishment could cause the random polarization resulting in multiple germ tube emergence sites.

The *arfB* mutant also displayed abnormal hyphal morphologies in the early stages of hyphal growth (hyphal lengths of less than 60 μm), in which the mutant often meandered off the long axis of polarity and branched dichotomously at hyphal apices, which may result from the loss of the ability to maintain polarity during hyphal growth (Fig. 3C). Hyphal growth to lengths of greater than 60 to 80 μm from conidia displayed almost wild-type like morphology, suggesting that the cell may mobilize another mechanism to compensate for the loss of ArfB, perhaps by upregulating one of the other five Arfs encoded by *A. nidulans*.

It is evident that disruption of the *arfB* gene resulted in deficiencies in bulk membrane internalization (Fig. 5) by endocytosis. The *arfB* mutant displayed a significant delay of FM4-64 uptake, and the efficiency of the dye uptake was lower than that seen for the wild type (Fig. 5). In addition, actin patches, which are considered to be clathrin-mediated endocytosis sites (26), were disrupted in apolar *arfB* mutant cells (Fig. 6A), suggesting that ArfB may be involved in clathrin-mediated endocytosis in *A. nidulans*. The clathrins have been shown to be recruited by Arf (26). Therefore, ArfB may play a role in recruiting the clathrins to the endocytosis site. An additional phenotype of the *arfB* mutant includes perturbation of endomembranes, which are less readily stained and have a diffuse appearance when perturbed (Fig. 5B). This phenomenon is similar to the perturbation of endomembranes in the human ARF6 mutant (39).

The polarization of exocytosis is generally accepted to be a key mechanism in polarized hyphal growth (3, 54). A role for endocytosis in the polarization of hyphae is, however, a relatively new concept. In pioneering work in the development of the endocytosis marker dye FM4-64 for filamentous fungi, Fischer-Parton and colleagues showed that endocytosis is an

ongoing process during hyphal growth (13). Steinberg has also addressed a role for endocytosis in the pathogenicity of *Ustilago maydis* (47). In three very recent studies, endocytosis has been incorporated into a model explaining hyphal growth (1, 48, 53). The endocytic markers FimA (53), AbpA, and SlaB (1) localize to a subapical collar in growing hyphae. Disruption of *fimA* resulted in a loss of endocytosis accompanied by severe cell polarity defects that produce phenotypes very similar to those for *arfB*::Tn as reported here (53). An apical tip growth apparatus model was recently proposed to combine both exocytic and endocytic mechanisms into a unified model for tip growth (48). An endocytic recycling model has also been proposed to explain the role of endocytosis in maintaining polarized membrane components at growing hyphal apices while recycling these components from the subapical region (53). This model accounts for the many varied hypotheses as to what the identity of polarized marker(s) is, including structural proteins, signaling proteins, ion channels, and lipid raft components. Takeshita and colleagues (49) have recently demonstrated the presence of TeaA and TeaR as cell end markers in *A. nidulans*. Could these proteins be maintained at the cell apex through endocytic recycling?

ArfB localized to plasma membranes and also appeared to localize to endomembranes (Fig. 6). This localization pattern needs to be interpreted with some caution, since the construct described here is both overexpressed via the *alcA* promoter and ectopically inserted. This localization pattern was, however, similar to that observed for human ARF6 (12, 39). In contrast, Arf3p in yeast is concentrated to the polarized budding site, though it localizes to peripheral membranes (22). The localization of ArfB to membranes depends on the myristoylation of the proteins. We have shown that mutation of the N-myristoylation motif changes the ArfB localization pattern to diffusion throughout the cytoplasm (Fig. 6). Similarly ArfB::GFP was diffuse in the *swoF* myristoylation mutant. Therefore, the loss of myristoylation of ArfB may explain in part the polarity defect previously reported for the NMT mutant (43).

ArfB localized to the plasma membrane and to endomembranes, but we did not observe it specifically concentrated to the hyphal apices. How then does ArfB take part in polarity establishment and maintenance? One model is that a protein which interacts with ArfB, such as its GDP/GTP exchange factor, concentrates to growing hyphal apices or its GTPase activation protein concentrates at sites away from the growing apex. A similar pattern has been observed for yeast where Bud1 (Rsr1), a *ras*-like GTPase, is required for bud site selection (8). The localization of Bud1p is cytosolic (23), but its GTPase activation protein, Bud2, localizes specifically to the bud sites (23).

In this paper, we have shown that ArfB plays a critical role in polarity establishment and maintenance. Hyphae tens of microns distal to the germ tube or branch initiation site grew as wild-type hyphae grow, suggesting that another gene may function to compensate for the absence of *arfB* or that the gene may function primarily during the initial stages of hyphal growth. At least one function of ArfB is in endocytosis, but whether its endocytosis function is through nucleating vesicle assembly or through participating in the organization of the actin cytoskeleton remains to be fully elucidated. N myristoylation of ArfB is critical for its proper localization. ArfB is only 1 of 41 proteins in the predicted myristoylome of *A. nidulans* (31). Therefore, further investigation will continue to elucidate the role of myristoylation in regulating cell development in *A. nidulans*.

ACKNOWLEDGMENTS

We are grateful to Dan Ebbole, Herman Scholthof, Deborah Bell-Pedersen, Srijana Upadhyay, and Dawoon Chung for invaluable discussions and critical reading of the manuscript. We are indebted to Rustem Omarov and Eun Young Huh for fruitful advice and insightful discussions about protein biochemistry.

S.C.L. was supported by a Nicholson fellowship and by a research assistantship from the Texas A&M University (TAMU) Department of Plant Pathology and Microbiology. This project was supported with startup funds to B.D.S. from the TAMU Department of Plant Pathology and Microbiology, the TAMU College of Agriculture and Life Science, and the Texas Agricultural Experiment Station.

REFERENCES

1. **Araujo-Bazan, L., M. A. Penalva, and E. A. Espeso.** 2008. Preferential localization of the endocytic internalization machinery to hyphal tips underlies polarization of the actin cytoskeleton in *Aspergillus nidulans*. Mol. Microbiol. **67:**891–905.
2. **Balch, W. E., R. A. Kahn, and R. Schwaninger.** 1992. ADP-ribosylation factor is required for vesicular trafficking between the endoplasmic reticulum and the *cis*-Golgi compartment. J. Biol. Chem. **267:**13053–13061.
3. **Bartnicki-Garcia, S.** 2002. Hyphal tip growth: outstanding questions. Marcel Dekker, New York, NY.
4. **Bartnicki-Garcia, S.** 2006. Chitosomes: past, present and future. FEMS Yeast Res. **6:**957–965.
5. **Bartnicki-Garcia, S., and E. Lippman.** 1969. Fungal morphogenesis: cell wall construction in *Mucor rouxii*. Science **165:**302–304.
6. **Bracker, C. E., J. Ruiz-Herrera, and S. Bartnicki-Garcia.** 1976. Structure and transformation of chitin synthetase particles (chitosomes) during microfibril synthesis *in vitro*. Proc. Natl. Acad. Sci. USA **73:**4570–4574.
7. **Bradke, F., and C. G. Dotti.** 1997. Neuronal polarity: vectorial cytoplasmic flow precedes axon formation. Neuron **19:**1175–1186.
8. **Cabib, E., J. Drgonova, and T. Drgon.** 1998. Role of small G proteins in yeast cell polarization and wall biosynthesis. Annu. Rev. Biochem. **67:**307–333.
9. **Costa, R., and K. R. Ayscough.** 2005. Interactions between Sla1p, Lsb5p and Arf3p in yeast endocytosis. Biochem. Soc. Trans. **33:**1273–1275.
10. **Costa, R., D. T. Warren, and K. R. Ayscough.** 2005. Lsb5p interacts with actin regulators Sla1p and Las17p, ubiquitin and Arf3p to couple actin dynamics to membrane trafficking processes. Biochem. J. **387:**649–658.
11. **D'Souza-Schorey, C., and P. Chavrier.** 2006. ARF proteins: roles in membrane traffic and beyond. Nat. Rev. Mol. Cell Biol. **7:**347–358.
12. **D'Souza-Schorey, C., G. Li, M. I. Colombo, and P. D. Stahl.** 1995. A regulatory role for ARF6 in receptor-mediated endocytosis. Science **267:**1175–1178.
13. **Fischer-Parton, S., R. M. Parton, P. C. Hickey, J. Dijksterhuis, H. A. Atkinson, and N. D. Read.** 2000. Confocal microscopy of FM4-64 as a tool for analysing endocytosis and vesicle trafficking in living fungal hyphae. J. Microsc. **198:**246–259.
14. **Flipphi, M., J. Kocialkowska, and B. Felenbok.** 2002. Characteristics of physiological inducers of the ethanol utilization (*alc*) pathway in *Aspergillus nidulans*. Biochem. J. **364:**25–31.
15. **Fuchs, U., G. Hause, I. Schuchardt, and G. Steinberg.** 2006. Endocytosis is essential for pathogenic development in the corn smut fungus *Ustilago maydis*. Plant Cell **18:**2066–2081.
16. **Giaever, G., A. M. Chu, L. Ni, C. Connelly, L. Riles, S. Veronneau, S. Dow, A. Lucau-Danila, K. Anderson, B. Andre, A. P. Arkin, A. Astromoff, M. El Bakkoury, R. Bangham, R. Benito, S. Brachat, S. Campanaro, M. Curtiss, K. Davis, A. Deutschbauer, K.-D. Entian, P. Flaherty, F. Foury, D. J. Garfinkel, M. Gerstein, D. Gotte, U. Guldener, J. H. Hegemann, S. Hempel, Z. Herman, D. F. Jaramillo, D. E. Kelly, S. L. Kelly, P. Kotter, D. LaBonte, D. C. Lamb, N. Lan, H. Liang, H. Liao, L. Liu, C. Luo, M. Lussier, R. Mao, P. Menard, S. L. Ooi, J. L. Revuelta, C. J. Roberts, M. Rose, P. Ross-Macdonald, B. Scherens, G. Schimmack, B. Shafer, D. D. Shoemaker, S. Sookhai-Mahadeo, R. K. Storms, J. N. Strathern, G. Valle, M. Voet, G. Volckaert, C.-Y. Wang, T. R. Ward, J. Wilhelmy, E. A. Winzeler, Y. Yang, G. Yen, E. Youngman, K. Yu, H. Bussey, J. D. Boeke, M. Snyder, P. Philippsen, R. W. Davis, and M. Johnston.** 2002. Functional profiling of the *Saccharomyces cerevisiae* genome. Nature **418:**387–391.
17. **Gillingham, A. K., and S. Munro.** 2007. The small G proteins of the Arf family and their regulators. Annu. Rev. Cell Dev. Biol. **23:**579–611.
18. **Girbardt, M.** 1957. Der Spitzenkörper von *Polystictus versicolor*. Planta **50:** 47–59.

19. **Grove, S. N., and C. E. Bracker.** 1970. Protoplasmic organization of hyphal tips among fungi: vesicles and Spitzenkörper. J. Bacteriol. **104:**989–1009.
20. **Harris, S. D., N. D. Read, R. W. Roberson, B. Shaw, S. Seiler, M. Plamann, and M. Momany.** 2005. Polarisome meets Spitzenkörper: microscopy, genetics, and genomics converge. Eukaryot. Cell **4:**225–229.
21. **Hicke, L., B. Zanolari, and H. Riezman.** 1998. Cytoplasmic tail phosphorylation of the alpha-factor receptor is required for its ubiquitination and internalization. J. Cell Biol. **141:**349–358.
22. **Huang, C.-F., Y.-W. Liu, L. Tung, C.-H. Lin, and F.-J. S. Lee.** 2003. Role for Arf3p in development of polarity, but not endocytosis, in *Saccharomyces cerevisiae*. Mol. Biol. Cell **14:**3834–3847.
23. **Huh, W.-K., J. V. Falvo, L. C. Gerke, A. S. Carroll, R. W. Howson, J. S. Weissman, and E. K. O'Shea.** 2003. Global analysis of protein localization in budding yeast. Nature **425:**686–691.
24. **Johnson, D. R., R. S. Bhatnagar, L. J. Knoll, and J. I. Gordon.** 1994. Genetic and biochemical studies of protein N-myristoylation. Annu. Rev. Biochem. **63:**869–914.
25. **Johnson, D. R., S. J. Cok, H. Feldmann, and J. I. Gordon.** 1994. Suppressors of nmt1-181, a conditional lethal allele of the *Saccharomyces cerevisiae* myristoyl-CoA:protein N-myristoyltransferase gene, reveal proteins involved in regulating protein N-myristoylation. Proc. Natl. Acad. Sci. USA **91:**10158–10162.
26. **Kaksonen, M., Y. Sun, and D. G. Drubin.** 2003. A pathway for association of receptors, adaptors, and actin during endocytic internalization. Cell **115:**475–487.
27. **Kaminskyj, S. G. W.** 2001. Fundamentals of growth, storage, genetics and microscopy of *Aspergillus nidulans*. Fungal Genet. Newsl. **48:**25–31.
28. **Kuo, K., and H. C. Hoch.** 1996. Germination of *Phyllosticta ampelicida* pycnidiospores: prerequisite of adhesion to the substratum and the relationship of substratum wettability. Fungal Genet. Biol. **20:**18–29.
29. **Laemmli, U. K.** 1970. Cleavage of structural proteins during the assembly of the head of bacteriophage T4. Nature **227:**680–685.
30. **Lambert, A. A., M. P. Perron, E. Lavoie, and D. Pallotta.** 2007. The *Saccharomyces cerevisiae* Arf3 protein is involved in actin cable and cortical patch formation. FEMS Yeast Res. **7:**782–795.
31. **Lee, S. C., and B. D. Shaw.** 2007. A novel interaction between N-myristoylation and the 26S proteasome during cell morphogenesis. Mol. Microbiol. **63:**1039–1053.
32. **Lee, S. C., and B. D. Shaw.** 2008. Localization and function of ADP ribosylation factor A in *Aspergillus nidulans*. FEMS Microbiol. Lett. **283:**216–222.
33. **Maurer-Stroh, S., B. Eisenhaber, and F. Eisenhaber.** 2002. N-terminal N-myristoylation of proteins: prediction of substrate proteins from amino acid sequence. J. Mol. Biol. **317:**541–557.
34. **Molendijk, A. J., B. Ruperti, and K. Palme.** 2004. Small GTPases in vesicle trafficking. Curr. Opin. Plant Biol. **7:**694–700.
35. **Moss, J., and M. Vaughan.** 1995. Structure and function of ARF proteins: activators of cholera toxin and critical components of intracellular vesicular transport processes. J. Biol. Chem. **270:**12327–12330.
36. **Moss, J., and M. Vaughan.** 1998. Molecules in the ARF orbit. J. Biol. Chem. **273:**21431–21434.
37. **Nayak, T., E. Szewczyk, C. E. Oakley, A. Osmani, L. Ukil, S. L. Murray, M. J. Hynes, S. A. Osmani, and B. R. Oakley.** 2006. A versatile and efficient gene-targeting system for *Aspergillus nidulans*. Genetics **172:**1557–1566.
38. **Penalva, M. A.** 2005. Tracing the endocytic pathway of *Aspergillus nidulans* with FM4-64. Fungal Genet. Biol. **42:**963–975.
39. **Peters, P. J., V. W. Hsu, C. E. Ooi, D. Finazzi, S. B. Teal, V. Oorschot, J. G. Donaldson, and R. D. Klausner.** 1995. Overexpression of wild-type and mutant ARF1 and ARF6: distinct perturbations of nonoverlapping membrane compartments. J. Cell Biol. **128:**1003–1017.
40. **Rosenwald, A. G., M. A. Rhodes, H. Van Valkenburgh, V. Palanivel, G. Chapman, A. Boman, C.-J. Zhang, and R. A. Kahn.** 2002. *ARL1* and membrane traffic in *Saccharomyces cerevisiae*. Yeast **19:**1039–1056.
41. **Rudnick, D. A., C. A. McWherter, G. W. Gokel, and J. I. Gordon.** 1993. MyristoylCoA:protein N-myristoyltransferase. Adv. Enzymol. Relat. Areas Mol. Biol. **67:**375–430.
42. **Sambrook, J., E. F. Fritsch, and T. Maniatis.** 1989. Molecular cloning: a laboratory manual. Cold Spring Harbor Laboratory Press, Cold Spring Harbor, NY.
43. **Shaw, B. D., C. Momany, and M. Momany.** 2002. *Aspergillus nidulans swoF* encodes an *N*-myristoyl transferase. Eukaryot. Cell **1:**241–248.
44. **Shaw, B. D., and S. Upadhyay.** 2005. *Aspergillus nidulans swoK* encodes an RNA binding protein that is important for cell polarity. Fungal Genet. Biol. **42:**862–872.
45. **Shevchenko, A., H. Tomas, J. Havlis, J. V. Olsen, and M. Mann.** 2006. In-gel digestion for mass spectrometric characterization of proteins and proteomes. Nat. Protoc. **1:**2856–2860.
46. **Stearns, T., R. A. Kahn, D. Botstein, and M. A. Hoyt.** 1990. ADP ribosylation factor is an essential protein in *Saccharomyces cerevisiae* and is encoded by two genes. Mol. Cell. Biol. **10:**6690–6699.
47. **Steinberg, G.** 2007. On the move: endosomes in fungal growth and pathogenicity. Nat. Rev. Microbiol. **5:**309–316.
48. **Taheri-Talesh, N., T. Horio, L. Araujo-Bazan, X. Dou, E. A. Espeso, M. A. Penalva, S. A. Osmani, and B. R. Oakley.** 2008. The tip growth apparatus of *Aspergillus nidulans*. Mol. Biol. Cell **19:**1439–1449.
49. **Takeshita, N., Y. Higashitsuji, S. Konzack, and R. Fischer.** 2008. Apical sterol-rich membranes are essential for localizing cell end markers that determine growth directionality in the filamentous fungus *Aspergillus nidulans*. Mol. Biol. Cell **19:**339–351.
50. **Taylor, L. P., and P. K. Hepler.** 1997. Pollen germination and tube growth. Annu. Rev. Plant Physiol. Plant Mol. Biol. **48:**461–491.
51. **Toews, M., J. Warmbold, S. Konzack, P. Rischitor, D. Veith, K. Vienken, C. Vinuesa, H. Wei, and R. Fischer.** 2004. Establishment of mRFP1 as a fluorescent marker in *Aspergillus nidulans* and construction of expression vectors for high-throughput protein tagging using recombination in vitro (GATEWAY). Curr. Genet. **45:**383–389.
52. **Upadhyay, S., and B. D. Shaw.** 2006. A phosphoglucose isomerase mutant in *Aspergillus nidulans* is defective in hyphal polarity and conidiation. Fungal Genet. Biol. **43:**739–751.
53. **Upadhyay, S., and B. D. Shaw.** 2008. The role of actin, fimbrin and endocytosis in growth of hyphae in *Aspergillus nidulans*. Mol. Microbiol. **68:**690–705.
54. **Virag, A., and S. D. Harris.** 2006. The spitzenkorper: a molecular perspective. Mycol. Res. **110:**4–13.
55. **Wedlich-Soldner, R., S. Altschuler, L. Wu, and R. Li.** 2003. Spontaneous cell polarization through actomyosin-based delivery of the Cdc42 GTPase. Science **299:**1231–1235.